Published in final edited form as:
Matrix Biol. 2014 April ; 35: 132–142. doi:10.1016/j.matbio.2013.12.003.

De novo expression of circulating biglycan evokes an innate inflammatory tissue response via MyD88/TRIF pathways

Jinyang Zeng-Brouwers[a,1], **Janet Beckmann**[a,1], **Madalina-Viviana Nastase**[a], **Renato V. Iozzo**[b], and **Liliana Schaefer**[a,*]

[a]Pharmazentrum Frankfurt, Institut für Allgemeine Pharmakologie und Toxikologie/ZAFES, Klinikum der Goethe-Universität, Frankfurt am Main, Germany

[b]Department of Pathology, Anatomy and Cell Biology, and the Cancer Cell Biology and Signaling Program, Kimmel Cancer Center, Thomas Jefferson University, Philadelphia, PA, USA

Abstract

Matrix-bound constituents, such as the small leucine-rich proteoglycan biglycan, can act as powerful signaling molecules when released by limited proteolysis of the extracellular matrix or *de novo* synthesized by macrophages in the circulation and body fluids. Specifically, biglycan acts as an endogenous ligand of innate immunity by directly engaging the Toll-like receptor (TLR)-2 and -4. In this study, we generated a transient transgenic mouse model where biglycan was *de novo* overproduced by hepatocytes driven by the albumin promoter. Transgenic biglycan was rapidly and abundantly synthesized by hepatocytes and released into the bloodstream. Notably, we found that circulating biglycan accumulated in the kidneys where it caused recruitment of leukocytes infiltrating the renal parenchyma concurrent with abnormal renal levels of chemoattractants CXCL1, CXCL2, CCL2 and CCL5. Using mice deficient in either TLR adapter proteins MyD88 or TRIF we discovered that MyD88 deficiency drastically reduced neutrophil and macrophage infiltration in the kidney, whereas TRIF deficiency decreased T cell infiltrates. Production of CXCL1, CXCL2 and CCL2 required MyD88, whereas the levels of T cell and macrophage attractant CCL5 required TRIF. Thus, we provide robust genetic evidence for circulating biglycan as a powerful pro-inflammatory mediator targeting the renal parenchyma. Furthermore, our results provide the first evidence that biglycan differentially triggers chemoattraction of leukocytes via two independent pathways, both under the control of TLR2/4, utilizing either MyD88 or TRIF adaptor proteins. As aberrant expression of biglycan occurs in several inflammatory diseases, this transient transgenic mouse model could serve as a valuable research tool in investigating the effects of increased biglycan expression *in vivo* and for the development of therapeutic strategies in the treatment of inflammatory diseases.

*Corresponding author: Liliana Schaefer, Pharmazentrum Frankfurt, Institut für Allgemeine Pharmakologie und Toxikologie, Klinikum der Goethe-Universität Frankfurt am Main, Haus 74, Z. 3.108a, Theodor-Stern-Kai 7, 60590 Frankfurt am Main, Germany, Fax: +49 69 6301 83027, Tel: +49 69 6301 7899, schaefer@med.uni-frankfurt.de.
[1]These authors contributed equally to this work.

Keywords

Extracellular matrix; Toll-like receptors; danger signal; macrophage; chemoattractants; innate immunity

1. Introduction

The small leucine-rich proteoglycan (SLRP) biglycan has a widespread distribution in the extracellular matrix of a large variety of tissues (Bianco et al., 1990). The biglycan molecule consists of a ~45-kDa protein core and one or two glycosaminoglycan (GAG) chains attached to the N-terminal region (Choi et al., 1989). Thought initially to have only a structural function (Fisher et al., 1983), it is now widely established that biglycan can play multiple biological roles (Nastase et al., 2012) that range from regulating bone formation and mass (Berendsen et al., 2011; Chen et al., 2002; Nikitovic et al., 2012; Parisuthiman et al., 2005; Xu et al., 1998; Young et al., 2002), stabilizing nerve-muscle synapses (Amenta et al., 2012) and the dystrophin-glycoprotein complex in muscle fibers (Bowe et al., 2000; Rafii et al., 2006) to serving as an endogenous molecule with a role in sterile and pathogen-mediated inflammation (Babelova et al., 2009; Frey et al., 2013; Iozzo, 2011; Kikuchi et al., 2000; Kitaya and Yasuo, 2009; Merline, 2012; Merline et al., 2009; Moreth et al., 2010; Moreth et al., 2012; Nastase et al., 2012; Popovic et al., 2011; Schaefer et al., 2005; Schaefer and Iozzo, 2008, 2012; Schaefer and Schaefer, 2010; Sjoberg et al., 2009).

In earlier studies performed on mouse peritoneal macrophages, biglycan was shown to act as an endogenous ligand of TLR2/4 following metalloprotease-mediated release from the extracellular matrix (Schaefer et al., 2005); in this role it is similar to the closely related decorin (Merline et al., 2011). In its soluble form, intact biglycan binds TLR2/4 and triggers the activation of p38/ERK and NF-κB followed by secretion of tumor necrosis factor (TNF)-α and CXCL2 (Schaefer et al., 2005). Additionally, soluble biglycan mediates the clustering of TLR2/4 with the purinergic $P2X_4/P2X_7$ receptors and triggers the assembly of NLRP3 inflammasome, followed by activation of caspase-1 and secretion of interleukin-1β (IL-1β) (Babelova et al., 2009). Notably, biglycan-null mice show an improved survival upon LPS-induced sepsis (Schaefer et al., 2005), and exhibit attenuated levels of active caspase-1 and mature IL-1β in response to either septic shock or non-infectious inflammatory renal injury (Babelova et al., 2009). In agreement with these experimental data, increased biglycan expression occurs in a number of pathogenic and sterile inflammatory conditions (Adapala et al., 2012; de Kluijver et al., 2005; Derbali et al., 2010; Moreth et al., 2010; Popovic et al., 2011; Schaefer et al., 2002; Westergren-Thorsson et al., 1993).

The goal of the present study was to investigate the pro-inflammatory mechanism of soluble (circulating) biglycan and elucidate the signaling pathways through which biglycan would elicit the production of chemoattractants and the recruitment of leukocytes. To this end, we generated a transient transgenic mouse model where full-length and fully glycanated biglycan was *de novo* synthesized by hepatocytes. We discovered that biglycan released in the circulation preferentially targeted the renal parenchyma with profound consequences. First, biglycan induced the sequential recruitment of neutrophils, macrophages and T lymphocytes. Second, circulating biglycan evoked the production of chemoattractants

CXCL1, CXCL2 and CCL2 in a TLR2/4/MyD88-dependent manner, whereas the production of CCL5 was TLR4/TRIF dependent. Based on the clinical observation that circulating biglycan is markedly increased in several infectious and sterile inflammatory processes, this transient transgenic mouse model could provide a new and useful investigative tool for studying the effects of increased biglycan expression *in vivo* and for the development of therapeutic strategies in the treatment of inflammatory diseases.

2. Results

2.1. De novo expression of soluble biglycan by transduced hepatocytes leads to its release in the bloodstream and distribution to the kidney

To investigate the *in vivo* pro-inflammatory effects and the signaling mechanisms triggered by soluble biglycan, we generated a mouse model by injecting intravenously a DNA construct containing human biglycan cDNA inserted into the *BamH*I/*Sac*II site of the pLIVE (Liver in Vivo Expression) vector. The pLIVE expression vector ensures liver-specific expression of exogenous proteins insofar as the transgene is driven by the powerful albumin promoter. To validate expression of human biglycan mRNA we analyzed h*BGN* mRNA expression levels in the transgenic livers by RT-PCR-RFLP at various intervals (1–14 days) post-injection (Fig. 1A). To distinguish the human from the endogenous mouse biglycan, we took advantage of a unique *Sac*I-sensitive site exclusively present in the human mRNA. When untreated, both human and mouse RT-PCR products encompass a 428-bp product; however, when digested with *Sac*I only the human mRNA is cleaved in two fragments of 165-bp and 272-bp (Fig. 1A). The results showed a rapid (1 day) expression of biglycan and this induction remained relatively constant for the first week post-injection, declining thereafter (Fig. 1A). There was no detectable human biglycan mRNA three weeks post-injection (not shown). In control mice injected with either vehicle or pLIVE vector, only endogenous mouse biglycan expression was observed four days post-injection. Notably, in all other investigated organs (including heart, lung, spleen, pancreas and brain) h*BGN* expression was totally undetectable (Fig. 1B). Importantly, liver function, measured by alkaline phosphatase, serum glutamic oxaloacetic transaminase and γ-glutamyl transpeptidase tests, was not affected by transfection of pLIVE-h*BGN* or empty vector and no antibodies against human biglycan could be detected in the circulation at any time-point (data not shown).

Collectively, these results show that the pLIVE system can support sustained transgene expression in the liver.

To corroborate the liver-specific nature of the pLIVE system, we utilized Hepa 1–6 cells and found that these cells were able to secrete a physiological, non-modified form of human biglycan (data not shown). Next, we determined the protein expression of biglycan in mouse liver at different time points (1–14 days) following pLIVE-h*BGN* injection. We extracted proteoglycans from liver homogenates and subsequently subjected them to Western blot analysis with and without chondroitinase ABC digestion for removal of the glycosaminoglycan chains. Notably, the transgenic livers contained higher levels of intact fully-glycanated biglycan as compared to either vehicle- or pLIVE-injected mice (Fig. 1C). Following chondroitinase ABC digestion, only biglycan protein core of 45-kDa was

detected in the liver of vehicle-, pLIVE- or pLIVE-h*BGN*-injected mice, with the samples from the latter showing a higher abundance of biglycan protein core (Fig. 1C). Time-course experiments showed a production of biglycan proteoglycan similar to the mRNA data, with peaks at 4 days post-injection, and a progressive decline at 7 and 14 days (Fig. 1D).

Next, we verified if biglycan overexpressed in the liver was actually reaching the blood circulation. To this end, we purified samples of plasma from animals injected with vehicle, pLIVE and pLIVE-h*BGN* at 1, 4, 7 and 14 days post-injection and digested with chondroitinase ABC. In agreement with the mRNA data shown above, we found that only after transfection with pLIVE-h*BGN*, biglycan was detected in the circulation, reaching maximal levels at 4 days post-injection (Fig. 1E).

Next, we examined if soluble biglycan released to plasma targeted the renal parenchyma. First, we isolated biglycan from kidneys of vehicle- and pLIVE-h*BGN*-injected mice and found high levels of human biglycan only in the latter samples (Fig. 1F). In addition, immunostaining for biglycan in renal sections from pLIVE and pLIVE-h*BGN*-injected mice showed robust accumulation of transgenic biglycan in both glomeruli and tubulointerstitium (Fig. 1G). Thus, the hepatic-generated human biglycan enters the circulation and targets specifically the renal parenchyma in this transient transgenic mouse model.

2.2. Overexpression of circulating biglycan evokes renal infiltration of immune cells in a determined temporal fashion concurrent production of chemoattractants

To investigate the inflammatory effects of h*BGN* overexpression *in vivo* we isolated cells from mouse kidneys and quantified by FACS the number of infiltrating leukocytes in pLIVE- and pLIVE-h*BGN*-injected mice at 1, 4, 7 and 14 days post-injection. At early time points post injection, a high influx of neutrophils (7/4+) was detected in the kidney. The 7/4+ cells reached maximal levels 1 day post-injection and then gradually decreased until 14 days when they reached the pLIVE control levels (Fig. 2A, red profile). Neutrophiles were located predominantly in glomeruli from mice overexpressing biglycan (immunostaining, Fig. S1). Using CD11b and F4/80 macrophage markers, we determined that the number of infiltrating macrophages concurrently increased in the kidneys of pLIVE-h*BGN* transgenic mice as compared to controls. The macrophage profile showed maximal levels at 4 days post-injection followed by a slow decrease. In comparison to neutrophils, the decrease in the number of macrophages was less pronounced as these cells were still detectable at high levels 14 days post-transfection (Fig. 2A, green profile). F4/80 positive cell infiltrates were detected in the tubulointerstitium of pLIVE-h*BGN*-injected mice (Fig. S1). Unlike the number of the infiltrating neutrophils and macrophages which peaked at earlier time points (1 and 4 days, respectively), the number of infiltrating T cells (CD3+) resulting after pLIVE-h*BGN* injection increased progressively during the entire duration of the experiment and remained significant also at 14 days (Fig. 2A, blue profile). CD3+ cells were found in glomeruli and the tubulointerstitium of pLIVE-h*BGN*-injected mice (Fig. S1). Figure 2 presents representative FACS plots showing the percentage of the 7/4+ (Fig. 2B), F4/80+CD11b+ (Fig. 2C), CD3+CD4+ (Fig. 2D) and CD3+CD8+ (Fig. 2E) cells in kidney at the time point corresponding to their respective maximum post-injection. Besides the

kidney, soluble biglycan was also able to induce immune cell infiltration in the lungs (Fig. S2).

Thus, overexpression of soluble biglycan induces renal infiltration by various immune cells following different kinetics.

2.3. Overexpression of circulating biglycan evokes renal production of chemoatranctants

To further investigate if soluble biglycan was driving the recruitment of leukocytes to the kidney by increasing the production of the respective chemokines, we analyzed *in vivo* the biglycan-induced expression of CXCL1, CXCL2, both responsible for the recruitment of neutrophils to the inflamed tissue, CCL2, chemoattractant for macrophages and CCL5, chemoattractant for macrophages and T cells. Given that the time profiles for the biglycan-mediated immune cell recruitment were distinct for each type of cells, we analyzed the chemokine expression at the same time points after pLIVE-h*BGN* injection as in the flow cytometric analysis. The mRNA level and protein abundance of CXCL1, CXCL2, CCL2 and CCL5 were measured in the kidneys of vehicle-, pLIVE- and pLIVE-h*BGN*-injected mice at 1, 4, 7 days post injection. At both the mRNA (Fig. 3A, C) and protein (Fig. 3B, D) levels, CXCL1 and CXCL2 were induced after 1 day, as consequence of soluble biglycan overexpression, declining thereafter and reaching levels similar to the controls at 7 days. Notably, the CXCL1 and CXCL2 expression profiles correlated with the early onset of neutrophil infiltration observed under these conditions (*cfr.* Fig. 2A).

Circulating human biglycan was also able to induce CCL2 expression in the kidney at 1 day post-injection. However, unlike CXCL1 and CXCL2, CCL2 mRNA and protein levels remained constant between 1 and 4 days and only significantly decreased at 7 days after pLIVE-h*BGN* injection though they were still induced compared to control level (Fig. 3E–F). CCL5 levels were also increased in the kidney of pLIVE-h*BGN*-transfected mice at 1 day post-injection compared to the control mice. However, at the mRNA levels (Fig. 3G) *Ccl5* expression remained constant for up to 7 days and CCL5 protein abundance (Fig. 3H) slightly increases after 1 day, in agreement with the T cell recruitment profile (*cfr.* Fig. 2A).

Collectively, our results indicate that the *in vivo* overexpression of circulating biglycan in mice induces the expression of specific renal chemokines responsible for the active recruitment of neutrophils, macrophages and T cells to the target organ.

2.4. Biglycan induces the production of CXCL1, CXCL2 and CCL2 in a TLR2/TLR4/MyD88-dependent manner and CCL5 by signaling through TLR4/TRIF in macrophages

To further investigate the cellular mechanism responsible for biglycan bioactivity, we isolated peritoneal macrophages from isogenic (C57BL/6) mice and stimulated them with recombinant human biglycan. After a four-h exposure to biglycan (4 μg/ml, 80 nM), mRNA levels of *Cxcl1*, *Cxcl2*, *Ccl2* and *Ccl5* were markedly induced (Fig. 4A, C, E, and G). The mRNA data were confirmed by quantification of the respective proteins in the supernatants of the cells measured after 16 h of continuous treatment with equimolar amounts of recombinant biglycan (Fig. 4B, D, F, and H). Collectively, these findings provide a mechanistic explanation for the *in vivo* data, that soluble biglycan recruits inflammatory

cells to the kidneys by inducing the production of various chemoattractants responsible for the progression of a cellular infiltrate and inflammation.

2.5. Involvement of TLR2/4, MyD88 and TRIF in the biglycan-induced secretion of chemokines

Next, we investigated the mechanism through which biglycan would induce CXCL1, CXCL2, CCL2 and CCL5. To this end, we isolated macrophages from C57BL/6, *Tlr2*$^{-/-}$, *Tlr4*$^{-/-}$ and *Tlr2*$^{-/-}$*Tlr4-m* mice and stimulated them for 16 h with recombinant human biglycan (80 nM). The results clearly show that biglycan signals through both the TLR2 and TLR4 receptors in order to induce the production of CXCL1, CXCL2 and CCL2 (Fig. 5A–C). Distinctly, biglycan induced the production of CCL5 through TLR4 but independently of TLR2 (Fig. 5D).

Signaling through TLR4 involves the formation of the LPS/MD2/TLR4 complex and the recruitment of MyD88 and TIRAP adaptors to the cytosolic domain of TLR4 leading to the early phase activation of NF-κB. However, the LPS/MD2/TLR4 complex is then internalized recruiting the TRAM and TRIF adaptors and leading to both the late phase activation of NF-kB and IRF3 activation. Distinctly, the TLR2 signaling pathway involves only MyD88 and TIRAP for the NF-κB activation (Kawai and Akira, 2010). Further, given that for their production in macrophages biglycan signals through both the TLR2 and TLR4 receptors, we investigated if only MyD88 could be involved in the downstream mechanism of biglycan-dependent CXCL1, CXCL2 and CCL2 or if TRIF was involved as well. For this, we isolated peritoneal macrophages from C57BL/6, *MyD88*$^{-/-}$, *TRIF-m* and *MyD88*$^{-/-}$*TRIF*$^{-/-}$ mice and stimulated them with equimolar amounts of biglycan for 16 h. The results showed that the biglycan-mediated production of CXCL1 (Fig. 5E), CXCL2 (Fig. 5F) and CCL2 (Fig. 5G) was strictly dependent on the presence of MyD88. In contrast to the other three chemoattractants, only CCL5 production was dependent on TLR4 (Fig. 5D). Next, we verified which of the two distinct downstream pathways of Tlr4 signaling was primarily responsible for this differential regulation. We discovered that that biglycan-mediated CCL5 increase was dependent on TRIF pathway but not MyD88 (Fig. 5H). These findings provide novel information for a dual regulation of biglycan emanating from a same set of innate immune receptors.

2.6. Circulating biglycan evokes chemokine production through MyD88- and TRIF-dependent pathways leading to renal recruitment of leukocytes

Having established distinct cellular pathway in biglycan signaling using primary macrophages with distinct genetic deficiency in toll-like receptors and their adaptor molecules, we next investigated the effects of soluble human biglycan overexpression *in vivo* in various mutant animals. Specifically, we injected the pLIVE-h*BGN* construct in C57BL/6, *MyD88*$^{-/-}$, *TRIF-m* and *MyD88*$^{-/-}$*TRIF*$^{-/-}$ mice. In agreement with the *in vitro*-based cellular studies, we confirmed that the production of CXCL1, CXCL2 and CCL2 in the kidney of pLIVE-h*BGN* transfected mice required the presence of the MyD88 adaptor. Indeed, *MyD88*$^{-/-}$ and *MyD88*$^{-/-}$*TRIF*$^{-/-}$ mice did not respond to circulating soluble biglycan (Fig. 6A–C). In contrast, in *TRIF-m* mice, the levels of CXCL1, CXCL2 and CCL2 after pLIVE-h*BGN* transfection were markedly elevated and comparable to the levels

obtained in wild-type C57BL/6 kidneys (Fig. 6A–C). Thus, the TRIF-dependent pathway is likely not involved in the biglycan-mediated production of the respective chemokines.

Notably, the production of the T cell and macrophage chemoattractant CCL5 following pLIVE-h*BGN* injection was markedly impaired in *TRIF-m* and *MyD88*$^{-/-}$/*TRIF*$^{-/-}$ mice (Fig. 6D). Thus, biglycan-mediated CCL5 production is TRIF-dependent in agreement with the results obtained with primary cultures of peritoneal macrophages (*cfr*. Fig. 5H). Slightly different from the *in vitro* results, when overexpressed in *MyD88*$^{-/-}$ mice, human biglycan induces CCL5 at higher levels compared to the levels from *TRIF-m* mice but slightly lower than in C57BL/6 mice (Fig. 6D).

2.7. Involvement of MyD88 and TRIF pathways in biglycan-mediated leukocyte recruitment to the kidneys

Having established the mechanism through which soluble biglycan induces the production of CXCL1, CXCL2, CCL2 and CCL5 *in vivo*, we next investigated whether this was the main cause for the recruitment of the respective immune cells to the kidney. Using a combination of specific immunological markers and FACS analysis, we quantified the number of neutrophils, macrophages and T cells infiltrated in the kidney of h*BGN* overexpressing C57BL/6, *MyD88*$^{-/-}$, *TRIF-m* and *MyD88*$^{-/-}$*TRIF*$^{-/-}$ mice. In accordance with the CXCL1 and CXCL2 production, we found that the recruitment of 7/4+ cells to the kidney was strictly dependent on the MyD88 pathway. Specifically, both *MyD88*$^{-/-}$ and *MyD88*$^{-/-}$*TRIF*$^{-/-}$ mice did not show any influx of 7/4+ cells to the kidney after injection of pLIVE-h*BGN*; in contrast, *TRIF-m* mice showed a marked elevation of newly recruited neutrophils comparable to the wild-type C57BL/6 kidneys (Fig. 7A–B). In agreement with the CCL2 production, we found that the number of F4/80+CD11b+ cells infiltrating the kidney was totally impaired in *MyD88*$^{-/-}$ and *MyD88*$^{-/-}$*TRIF*$^{-/-}$ mice (Fig. 7D), revealing MyD88 as the principal adaptor in the biglycan-mediated macrophage recruitment. In contrast, in *TRIF-m* mice, the influx of macrophages into the kidney was significantly high compared to the control but, unlike the CCL2 production profile (*cfr*. Fig. 6C), we observed a significant reduction in macrophage infiltration compared to C57BL/6 mice (Fig. 7D).

Finally, we examined the mechanism of biglycan-mediated T cell recruitment in the kidney by quantifying the number of CD3+CD4+ and CD3+CD8+ cells after pLIVE-h*BGN* injection (Fig. 7E). CD3+CD4+ cells were significantly recruited to the kidney following overexpression of soluble biglycan in C57BL/6 and *MyD88*$^{-/-}$ mice, while *TRIF-m* and *MyD88*$^{-/-}$*TRIF*$^{-/-}$ mice did not show any induction of T cell numbers (Fig. 7F). However, similar to CCL5, we observed a decrease in the number of CD3+CD4+ cells in *MyD88*$^{-/-}$ mice compared to C57BL/6 mice (Fig. 7F). Similar results were obtained for CD3+CD8+ cells (data not shown).

These findings emphasize the requirement of the TRIF adaptor protein for the production of CCL5 and recruitment of T cells in the kidney.

3. Discussion

In the present report we investigated the effects of soluble human biglycan overexpression in mice and thereby characterized in detail a transient transgenic mouse model generated by injection of the recombinant construct pLIVE-h*BGN* containing the human biglycan gene, h*BGN*, cloned into the pLIVE expression vector. We showed that h*BGN* mRNA is overexpressed specifically in the liver and that intact biglycan protein can be produced in the liver following overexpression. Soluble human biglycan is then released into the bloodstream where it specifically targets the kidneys. According to our working model (Fig. 8), once in the renal parenchyma, soluble biglycan triggers the synthesis and production of several chemoattractants such as CXCL1, CXCL2, CCL2 and CCL5 and consequently leads to the recruitment of neutrophils, macrophages and T cells. Our model also provides a mechanistic explanation for the recruitment of inflammatory cells to the kidneys, that is, a biglycan–evoked chemoattractant secretion by a direct protein/receptor interaction with macrophages, the key inflammatory cell responsible for biglycan signaling. This hypothesis is based on our cellular studies where we found that biglycan can act on mouse peritoneal macrophages as an inducer of CXCL1, CXCL2 and CCL2 secretion by signaling through the TLR2/4 receptors, a process which is MyD88 dependent. On the other hand biglycan is able to induce CCL5 in mouse macrophages by signaling in a TLR4- and TRIF-dependent manner. The end result of this interaction is that neutrophils, macrophages and T cells are rapidly and efficiently recruited to the kidneys completing the picture of the biglycan-mediated pro-inflammatory phenotype (Fig. 8). Indeed, it is now becoming evident that overproduction of circulating and soluble biglycan is a hallmark of several pathological situations leading to enhancement and perpetuation of inflammation.

In this study, we generated a transient transgenic mouse model mimicking inflammatory conditions by using a liver specific expression system, leading to a release of soluble biglycan. A transient expression of soluble biglycan was chosen in order to minimize compensatory effects in the mice. We found specifically in liver high levels of h*BGN* mRNA in the pLIVE-h*BGN*-injected mice. Notably, both mRNA and protein levels remained elevated for a full week post-transduction and could be detected as far as two weeks. This liver-specific expression correlated with the presence of high levels of soluble biglycan in the plasma of h*BGN*-overexpressing mice, proving that biglycan is able to be released into the bloodstream following overexpression in liver. Time-course experiments showed that at day 4 the level of biglycan protein in liver and plasma reached the highest abundance. In comparison, MRL/*lpr* mice show maximal biglycan levels in liver and plasma at day 7 post-injection (Moreth et al., 2010). At day 4 post-injection, we found high levels of biglycan in kidneys, in particular in the glomerulus and in the tubulointerstitium, suggesting that from the circulation soluble biglycan deposited to renal parenchyma. Therefore this *in vivo* model constitutes a useful tool for studying the involvement of soluble biglycan in the pathology of different renal diseases.

Our study provides the first evidence for a direct role of circulating biglycan in the renal recruitment of neutrophils. The infiltration of neutrophils was very rapid and peaked already at day 1 after transfection. Notably, the biglycan-induced renal infiltration of macrophages started at day 1 post transfection and peaked at day 4, whereas the infiltration of T cells was

observed after 4 days and remained continuously elevated for about 14 days post-transfection. Thus, biglycan evokes a dynamic inflammatory cell recruitment with a time-course similar to that obtained for the mRNA and protein levels of their respective chemoattractants. Specifically, we tested: (a) CXCL1 and CXCL2, well known recruiters of neutrophils, acting on their receptor CXCR2 (Roche et al., 2007), (b) CCL2, known to attract monocytes and tissue macrophages upon its release and interaction with CCR2 receptor (Tesch, 2008) and (c) CCL5 which can attract T cells, macrophages, natural killer cells, basophils and eosinophils (Krensky and Ahn, 2007). Notably, biglycan induces the chemokines CXCL1 and CXCL2 via TLR2/4 receptors and this induction is mediated via the MyD88 pathway. This is in accordance with observations made for the TLR4 ligand, LPS in bone marrow macrophages, as also here these chemokines were mainly induced via MyD88 (De Filippo et al., 2008). Interestingly, in the mentioned study, CXCL2 but not CXCL1 was additionally induced via a TRIF-dependent pathway. This was not the case in our study, however in MyD88-deficient macrophages CXCL2 was slightly but significantly induced by biglycan stimulation, indicating that also to the complete absence of the MyD88 adaptor, biglycan can still induce CXCL2 expression. De Felippo et al. further showed that application of LPS can induce neutrophil recruitment into the peritoneum also in MyD88-deficient mice. This was not the case for biglycan-induced renal neutrophil infiltration. Thus, we conclude that biglycan-mediated CXCL2 induction and the subsequent neutrophil recruitment are dependent on MyD88 pathway to an extent higher than that required by LPS. This could be due to the additional signaling of biglycan via TLR2. Importantly, a role in the recruitment of neutrophils has also been reported for hyaluronan, another endogenous ligand of TLR2 and TLR4 (Jiang et al., 2005).

The biglycan-induced renal expression of chemokine CCL2 and subsequent recruitment of macrophages to the kidney also showed a clear dependency on MyD88. This is in accordance with observations made in MyD88-deficient mice which show a marked reduction in macrophage infiltration in a model of renal ischemic damage (Wu et al., 2007). Interestingly, recruitment of macrophages induced by soluble biglycan in TRIF-deficient mice was less pronounced than in wild-type mice transfected with pLIVE-h*BGN*, even though both are completely dependent on the MyD88 pathway. This could be due to the fact that chemokine CCL5, which was induced by biglycan in a TRIF-dependent manner, is also able to recruit macrophages and not only T cells (Schall et al., 1990).

We observed that *in vitro* the induction of CCL5 was only dependent on the TRIF pathway, *in vivo* also pLIVE-h*BGN* transfected MyD88-deficient mice showed a reduction of renal CCL5 abundance compared to identically-treated wild-type mice. This observation could be explained by the reduced biglycan-mediated recruitment of macrophages to the kidney in MyD88-deficient mice, thereby reducing the source of CCL5 production. The biglycan-mediated recruitment of T cells to the kidney was mainly dependent on the TRIF pathway, in accordance with the observation made for the LPS induced recruitment of T cells to non-lymphatic tissues *in vivo* (McAleer et al., 2009). Interestingly, soluble biglycan was able to induce both $CD4^+$ T helper cells as well as $CD8^+$ cytotoxic T cells to the kidney. $CD4^+$ cells can be further distinguished into different Th cell subsets, e.g. Th1, Th2, Th17, Th22 or Tregs, all playing an important role in inflammation. It is tempting to speculate that under

pathological situations soluble biglycan could enhance the recruitment of specific Th subsets, thereby further driving disease progression.

In conclusion, we provide robust genetic evidence for circulating biglycan as a powerful pro-inflammatory SLRP preferentially targeting the renal glomeruli and tubulointerstitium. Thus, hepatocyte-derived expression of fully glycanated biglycan provides a viable animal model to study inflammation. Moreover, our results indicate that biglycan could be an interesting target for anti-inflammatory therapy. The identification of the underlying pathways leading to the recruitment of the different cells could help understanding the potential role of biglycan and perhaps other SLRPs during septic and aseptic inflammation.

4. Experimental procedures

4.1. Animal experiments

All animal work was conducted in accordance with the German Animal Protection Law and was approved by the Ethics Review Committee for laboratory animals of the District Government of Darmstadt, Germany. 8 week old male C57BL/6 mice were purchased from Charles River Laboratories (Sulzfeld, Germany). *TRIF-m* (*TRIF*$^{lps2/lps2}$) mice, *MyD88*$^{-/-}$ mice and *MyD88*$^{-/-}$*TRIF*$^{-/-}$ mice were provided by Prof. H.H. Radeke (Goethe University Frankfurt, Frankfurt, Germany), Prof. T. Miethke and Prof. K. Wagner (both from the Technical University of Munich, Munich, Germany) respectively. *Tlr2*$^{-/-}$ and *Tlr4*$^{-/-}$ mice were generously provided by Dr. M. Freudenberg (Max Planck Institute for Immunology, Freiburg, Germany). *Tlr2*$^{-/-}$*Tlr4-m* (*Tlr2*$^{-/-}$ mice with a mutation in *Tlr4* gene) mice were generously provided by Prof. C. Kirschning (Technical University of Munich, Munich, Germany).

4.2. Cell culture and stimulation

Macrophages were harvested by peritoneal lavage 5 days after injection of thioglycollate and cultured in RPMI 1640 (Life Technologies, Darmstadt, Germany) under serum-free conditions as described previously (Schaefer et al., 2005). Cells were stimulated with intact biglycan (4 μg/ml, 80 nM) for 4 h or 16 h.

4.3. Construction of the pLIVE-hBGN plasmid

The eukaryotic *in vivo* expression vector pLIVE containing the minimal mouse albumin promoter and the mouse alpha fetoprotein enhancer II was purchased from Mirus Bio (Madison, USA). Total RNA was extracted from human kidney cortex using the RNeasy Mini Kit (QIAGEN, Hilden, Germany). The open reading frame of human biglycan was amplified by RT-PCR using the Verso cDNA Synthesis Kit (Thermo Fisher Scientific, Schwerte, Germany). Primers used for h*BGN* amplification were 5′-TGA CAG GAT CCG CCA TGT GGC CCC TGT GGC GCC TC-3′ (forward) and 5′-AGT CCG CGG CTA CTT TTT GTA GTT GCC-3′ (reverse). The restriction sites for *BamH*I and *Sac*II were included in the forward and reverse primers, respectively for subsequent cloning. After restriction enzyme digestion with *BamH*I and *Sac*II (New England Biolabs, Frankfurt am Main, Germany), the amplified h*BGN* fragment was cloned into the pLIVE plasmid downstream of the first intron to generate the plasmid pLIVE-h*BGN*. The correct sequence was confirmed

by DNA sequencing. Large scale preparation of endotoxin-free pLIVE-h*BGN* was performed using the EndoFree Plasmid Maxi Kit (QIAGEN, Hilden, Germany).

4.4. Analysis of transgene expression by RT-PCR-RFLP

Total RNA extraction from mouse organs and semi-quantictative RT-PCR were performed as described previously (Fisher et al., 1991). The primers used were 5′-TGG AGA ACA GTG GCT TTG AA-3′ (forward) and 5′-ACT ACA ACG GCA TCA GCC TC-3′ (reverse), corresponding to a region of identity between the sequence of human and mouse biglycan cDNA and spanning several introns in the genomic sequence. Distinction between amplified human biglycan and endogenous mouse biglycan cDNA was done by digestion with *Sac*I (New England Biolabs, Frankfurt am Main, Germany), as the sequence amplified for *hBGN* contains an internal *Sac*I restriction site. Digestion of the amplified transcripts with *Sac*I results in two DNA fragments for human biglycan (272-bp and 165-bp) and one fragment (428-bp) for endogenous mouse biglycan.

4.5. In vivo transfection

For intravenous delivery, 80 μg of pLIVE-*hBGN* were incubated for 15 minutes before injection in sterile filtered 5% glucose solution containing ExGen 500 reagent (Thermo Fisher Scientific, Schwerte, Germany) at a ratio of 6 equivalents reagent/1 μg DNA. Intravenous injections were performed with a 30 Gauge needle, on isofluoran (Abbott Laboratories, Wiesbaden, Germany) anaesthetized mice. Mice were kept warm and monitored until recovery on a heat pad. Mice were euthanized at indicated time points after injection, for collection of blood and organs.

4.6. Real-time PCR of chemokines

Total RNA from macrophages and mouse organs was isolated using TRI Reagent (Sigma Aldrich, Hamburg, Germany) as described previously (Schaefer et al., 2001) and reverse transcribed using the Verso cDNA Synthesis Kit (Thermo Fisher Scientific, Schwerte, Germany).

cDNA was amplified using TaqMan Gene Expression Assays. Probes for *Gapdh* (Mm03302249_g1), *Cxcl1* (Mm00433850_m1), *Cxcl2* (Mm00436450_m1), *Ccl2* (Mm00441242_m1) and *Ccl5* (Mm01302428_m1) were purchased from Life Technologies (Darmstadt, Germany). Amplification and detection were performed with an ABI prism 7500 Sequence Detection System (Life Technologies, Darmstadt, Germany). Each sample was run in triplicate and the threshold cycle for the gene of interest was normalized to that of *Gapdh*.

4.7. Proteoglycan isolation and Western blot

Proteoglycans were isolated from plasma and organs as described previously (Schaefer et al., 2000; Schaefer et al., 2001). If required the proteoglycans were digested with chondroitinase ABC (Seikagaku, Tokyo, Japan) to remove glycosaminoglycan chains and subjected to polyacrylamide gel electrophoresis followed by Western blotting. Western blots were performed and quantified as described previously (Schaefer et al., 2001). Protein bands were visualized using ECL Plus Western Blotting Detection Reagents (GE Healthcare,

Freiburg, Germany). An antibody against the C-terminus of human biglycan (Acris Antibodies, Herford, Germany) and an anti-β-actin antibody (Sigma Aldrich, Hamburg, Germany) were used as primary antibodies.

4.8. ELISA

Protein levels of CXCL1, CXCL2, CCL2 and CCL5 were measured in culture media from mouse peritoneal macrophages and tissue lysates from mouse kidney using mouse-specific ELISA kits for the respective proteins (R&D Systems, Wiesbaden, Germany). Tissues were lysed in 20 mM Tris/HCl, pH 8, containing 137 mM NaCl, 5 mM EDTA, 10% Glycerol, 1% Triton-X 100, 1 mM dithiothreitol and 1 mM PMSF. After a short ultrasonication, samples were centrifuged and the supernatant was used for ELISA. Results were normalized to total protein content, determined using BCA Protein Assay Reagent (Thermo Fisher Scientific, Schwerte, Germany).

4.9. Immunohistochemistry

Serial sections (3 μm) of formaldehyde fixed, paraffin-embedded samples were processed for immunohistochemical studies by the alkaline phosphatase anti–alkaline phosphatase (APAAP) or horseradish peroxidase (HRP) and 3,3′-Diaminobenzidine techniques (Schaefer et al., 2002). Primary antibodies: goat anti-C-terminus of human biglycan (Acris Antibodies, Herford, Germany), rat anti-mouse F4/80 (Serotec), rat anti-mouse 7/4 (Abcam) and rat-anti mouse CD3 (Santa Cruz Biotechnology) were used. Incubation with the primary antibody was performed overnight at 4°C. The specificity of immunostaining was confirmed by omitting the primary antibody and by using non-immune serum / unspecific IgG. Counterstaining was performed with Mayer's Hematoxylin (Sigma). Infiltrating mononuclear cells were counted in a minimum of 15 randomly selected non-overlapping high-power fields (hpf 400x) of tissue sections. The number of neutrophils, macrophages and T cells was estimated per field (hpf 400x, with a minimum of 15 fields counted) (Soft Imaging System, Olympus). Sections were examined by a blinded observer.

4.10. Flow cytometry of renal cells

Kidneys were mechanically disrupted and digested for 45 min in 5 ml of 0.5 mg/ml Collagenase A (Roche, Mannheim, Germany) in DMEM with 10% FCS at 37°C. After repetitive pipetting, the tissue homogenates were sieved through a 70 μm filter (BD, Heidelberg, Germany). Red blood cells were lysed using ACK Buffer (0.15 M NH_4Cl, 10 mM $KHCO_3$, 0.1 mM Na_2EDTA) and cells washed with FACS buffer (1% FCS, 0.1% NaN_3 in PBS). Aliquots of the cell suspension were incubated with anti-CD16/32 ($FC\gamma$ RIII/II) antibody (BD, Heidelberg, Germany) followed by staining with the following antibodies: rat anti-mouse neutrophil, 7/4 (AbCam, Cambridge, UK), CD11b-APC (BD, Heidelberg, Germany), F4/80-PE, CD4, CD8, CD3-PerCP (all from eBiosciences, Frankfurt, Germany). For detection of neutrophil marker secondary FITC labeled rabbit anti-rat antibody was used. Samples were analyzed using a FACSCanto II flow cytometer (BD, Heidelberg, Germany).

4.11. Statistics

Data are presented as mean ± SEM for the *in vivo* data and ± SD for the *in vitro* data and analyzed by one-way analysis of variance (ANOVA) with Dunnett's significance test. Differences were considered significant at p-values<0.05.

Supplementary Material

Refer to Web version on PubMed Central for supplementary material.

Acknowledgments

This work was supported by the German Research Council (SFB 815, project A5, SFB 1039, project B2, and Excellence Cluster ECCPS to LS), LOEWE program Ub-Net (LS) and by NIH grants RO1 CA39481, RO1 CA47282 and RO1 CA164462 (RVI).

Abbreviations

CCL	chemokine (C-C motif) ligand
CCR2	C-C chemokine receptor type 2
CXCL	neutrophil chemoattractant chemokine C-X-C motif ligand
CXCR2	receptor C-X-C chemokine receptor type 2
FACS	fluorescence-activated cell sorting
IL-1β	interleukin-1β
LPS	lipopolysaccharide
MyD88	myeloid differentiation primary response 88
NF-κB	nuclear factor kappa-light-chain enhancer of activated B cells
NLRP3	NLR family, pyrin domain-containing 3
RFLP	restriction fragment length polymorphism
SLRP	small leucine-rich proteoglycans
TLR	Toll-like receptor
TRIF	TIR domain-containing adapter inducing interferon β

References

Adapala VJ, Ward M, Ajuwon KM. Adipose tissue biglycan as a potential anti-inflammatory target of sodium salicylate in mice fed a high fat diet. J Inflamm (Lond). 2012; 9:15. [PubMed: 22533381]

Amenta AR, Creely HE, Mercado ML, Hagiwara H, McKechnie BA, Lechner BE, Rossi SG, Wang Q, Owens RT, Marrero E, Mei L, Hoch W, Young MF, McQuillan DJ, Rotundo RL, Fallon JR. Biglycan is an extracellular MuSK binding protein important for synapse stability. J Neurosci. 2012; 32:2324–2334. [PubMed: 22396407]

Babelova A, Moreth K, Tsalastra-Greul W, Zeng-Brouwers J, Eickelberg O, Young MF, Bruckner P, Pfeilschifter J, Schaefer RM, Grone HJ, Schaefer L. Biglycan, a danger signal that activates the NLRP3 inflammasome via toll-like and P2X receptors. J Biol Chem. 2009; 284:24035–24048. [PubMed: 19605353]

Berendsen AD, Fisher LW, Kilts TM, Owens RT, Robey PG, Gutkind JS, Young MF. Modulation of canonical Wnt signaling by the extracellular matrix component biglycan. Proc Natl Acad Sci U S A. 2011; 108:17022–17027. [PubMed: 21969569]

Bianco P, Fisher LW, Young MF, Termine JD, Robey PG. Expression and localization of the two small proteoglycans biglycan and decorin in developing human skeletal and non-skeletal tissues. J Histochem Cytochem. 1990; 38:1549–1563. [PubMed: 2212616]

Bowe MA, Mendis DB, Fallon JR. The small leucine-rich repeat proteoglycan biglycan binds to alpha-dystroglycan and is upregulated in dystrophic muscle. J Cell Biol. 2000; 148:801–810. [PubMed: 10684260]

Chen XD, Shi S, Xu T, Robey PG, Young MF. Age-related osteoporosis in biglycan-deficient mice is related to defects in bone marrow stromal cells. J Bone Miner Res. 2002; 17:331–340. [PubMed: 11811564]

Choi HU, Johnson TL, Pal S, Tang LH, Rosenberg L, Neame PJ. Characterization of the dermatan sulfate proteoglycans, DS-PGI and DS-PGII, from bovine articular cartilage and skin isolated by octyl-sepharose chromatography. J Biol Chem. 1989; 264:2876–2884. [PubMed: 2914936]

De Filippo K, Henderson RB, Laschinger M, Hogg N. Neutrophil chemokines KC and macrophage-inflammatory protein-2 are newly synthesized by tissue macrophages using distinct TLR signaling pathways. J Immunol. 2008; 180:4308–4315. [PubMed: 18322244]

de Kluijver J, Schrumpf JA, Evertse CE, Sont JK, Roughley PJ, Rabe KF, Hiemstra PS, Mauad T, Sterk PJ. Bronchial matrix and inflammation respond to inhaled steroids despite ongoing allergen exposure in asthma. Clin Exp Allergy. 2005; 35:1361–1369. [PubMed: 16238797]

Derbali H, Bosse Y, Cote N, Pibarot P, Audet A, Pepin A, Arsenault B, Couture C, Despres JP, Mathieu P. Increased biglycan in aortic valve stenosis leads to the overexpression of phospholipid transfer protein via Toll-like receptor 2. Am J Pathol. 2010; 176:2638–2645. [PubMed: 20382708]

Fisher LW, Heegaard AM, Vetter U, Vogel W, Just W, Termine JD, Young MF. Human biglycan gene. Putative promoter, intron-exon junctions, and chromosomal localization. J Biol Chem. 1991; 266:14371–14377. [PubMed: 1860845]

Fisher LW, Termine JD, Dejter SW Jr, Whitson SW, Yanagishita M, Kimura JH, Hascall VC, Kleinman HK, Hassell JR, Nilsson B. Proteoglycans of developing bone. J Biol Chem. 1983; 258:6588–6594. [PubMed: 6189828]

Frey H, Schroeder N, Manon-Jensen T, Iozzo RV, Schaefer L. Biological interplay between proteoglycans and their innate immune receptors in inflammation. FEBS J. 2013

Iozzo, RV.; Goldoni, S.; Berendsen, A.; Young, M. Small leucine-rich proteoglycans. In: Mecham, RP., editor. The Extracellular Matrix: an Overview. Springer; New York: 2011. p. 197-266.

Jiang D, Liang J, Fan J, Yu S, Chen S, Luo Y, Prestwich GD, Mascarenhas MM, Garg HG, Quinn DA, Homer RJ, Goldstein DR, Bucala R, Lee PJ, Medzhitov R, Noble PW. Regulation of lung injury and repair by Toll-like receptors and hyaluronan. Nat Med. 2005; 11:1173–1179. [PubMed: 16244651]

Kawai T, Akira S. The role of pattern-recognition receptors in innate immunity: update on Toll-like receptors. Nat Immunol. 2010; 11:373–384. [PubMed: 20404851]

Kikuchi A, Tomoyasu H, Kido I, Takahashi K, Tanaka A, Nonaka I, Iwakami N, Kamo I. Haemopoietic biglycan produced by brain cells stimulates growth of microglial cells. J Neuroimmunol. 2000; 106:78–86. [PubMed: 10814785]

Kitaya K, Yasuo T. Dermatan sulfate proteoglycan biglycan as a potential selectin L/CD44 ligand involved in selective recruitment of peripheral blood CD16(−) natural killer cells into human endometrium. J Leukoc Biol. 2009; 85:391–400. [PubMed: 19088176]

Krensky AM, Ahn YT. Mechanisms of disease: regulation of RANTES (CCL5) in renal disease. Nat Clin Pract Nephrol. 2007; 3:164–170. [PubMed: 17322928]

McAleer JP, Rossi RJ, Vella AT. Lipopolysaccharide potentiates effector T cell accumulation into nonlymphoid tissues through TRIF. J Immunol. 2009; 182:5322–5330. [PubMed: 19380779]

Merline R, Moreth K, Beckmann J, Nastase MV, Zeng-Brouwers J, Tralhao JG, Lemarchand P, Pfeilschifter J, Schaefer RM, Iozzo RV, Schaefer L. Signaling by the matrix proteoglycan decorin controls inflammation and cancer through PDCD4 and MicroRNA-21. Sci Signal. 2011; 4:ra75. [PubMed: 22087031]

Merline, R.; Nastase, M.; Iozzo, RV.; Schaefer, L. Small leucine-rich proteoglycans: Multifunctional signaling effectors. In: Karamanos, NK., editor. Extracellular Matrix: Pathobiology and Signaling. DE GRUYTER; Berlin: 2012. p. 185-196.

Merline R, Schaefer RM, Schaefer L. The matricellular functions of small leucine-rich proteoglycans (SLRPs). J Cell Commun Signal. 2009; 3:323–335. [PubMed: 19809894]

Moreth K, Brodbeck R, Babelova A, Gretz N, Spieker T, Zeng-Brouwers J, Pfeilschifter J, Young MF, Schaefer RM, Schaefer L. The proteoglycan biglycan regulates expression of the B cell chemoattractant CXCL13 and aggravates murine lupus nephritis. J Clin Invest. 2010; 120:4251–4272. [PubMed: 21084753]

Moreth K, Iozzo RV, Schaefer L. Small leucine-rich proteoglycans orchestrate receptor crosstalk during inflammation. Cell Cycle. 2012; 11:2084–2091. [PubMed: 22580469]

Nastase MV, Young MF, Schaefer L. Biglycan: a multivalent proteoglycan providing structure and signals. J Histochem Cytochem. 2012; 60:963–975. [PubMed: 22821552]

Nikitovic D, Aggelidakis J, Young MF, Iozzo RV, Karamanos NK, Tzanakakis GN. The biology of small leucine-rich proteoglycans in bone pathophysiology. J Biol Chem. 2012; 287:33926–33933. [PubMed: 22879588]

Parisuthiman D, Mochida Y, Duarte WR, Yamauchi M. Biglycan modulates osteoblast differentiation and matrix mineralization. J Bone Miner Res. 2005; 20:1878–1886. [PubMed: 16160746]

Popovic ZV, Wang S, Papatriantafyllou M, Kaya Z, Porubsky S, Meisner M, Bonrouhi M, Burgdorf S, Young MF, Schaefer L, Grone HJ. The proteoglycan biglycan enhances antigen-specific T cell activation potentially via MyD88 and TRIF pathways and triggers autoimmune perimyocarditis. J Immunol. 2011; 187:6217–6226. [PubMed: 22095710]

Rafii MS, Hagiwara H, Mercado ML, Seo NS, Xu T, Dugan T, Owens RT, Hook M, McQuillan DJ, Young MF, Fallon JR. Biglycan binds to alpha- and gamma-sarcoglycan and regulates their expression during development. J Cell Physiol. 2006; 209:439–447. [PubMed: 16883602]

Roche JK, Keepers TR, Gross LK, Seaner RM, Obrig TG. CXCL1/KC and CXCL2/MIP-2 are critical effectors and potential targets for therapy of Escherichia coli O157:H7-associated renal inflammation. Am J Pathol. 2007; 170:526–537. [PubMed: 17255321]

Schaefer L, Babelova A, Kiss E, Hausser HJ, Baliova M, Krzyzankova M, Marsche G, Young MF, Mihalik D, Gotte M, Malle E, Schaefer RM, Grone HJ. The matrix component biglycan is proinflammatory and signals through Toll-like receptors 4 and 2 in macrophages. J Clin Invest. 2005; 115:2223–2233. [PubMed: 16025156]

Schaefer L, Grone HJ, Raslik I, Robenek H, Ugorcakova J, Budny S, Schaefer RM, Kresse H. Small proteoglycans of normal adult human kidney: distinct expression patterns of decorin, biglycan, fibromodulin, and lumican. Kidney Int. 2000; 58:1557–1568. [PubMed: 11012890]

Schaefer L, Iozzo RV. Biological functions of the small leucine-rich proteoglycans: from genetics to signal transduction. J Biol Chem. 2008; 283:21305–21309. [PubMed: 18463092]

Schaefer L, Iozzo RV. Small leucine-rich proteoglycans, at the crossroad of cancer growth and inflammation. Curr Opin Genet Dev. 2012; 22:56–57. [PubMed: 22326829]

Schaefer L, Macakova K, Raslik I, Micegova M, Grone HJ, Schonherr E, Robenek H, Echtermeyer FG, Grassel S, Bruckner P, Schaefer RM, Iozzo RV, Kresse H. Absence of decorin adversely influences tubulointerstitial fibrosis of the obstructed kidney by enhanced apoptosis and increased inflammatory reaction. Am J Pathol. 2002; 160:1181–1191. [PubMed: 11891213]

Schaefer L, Raslik I, Grone HJ, Schonherr E, Macakova K, Ugorcakova J, Budny S, Schaefer RM, Kresse H. Small proteoglycans in human diabetic nephropathy: discrepancy between glomerular expression and protein accumulation of decorin, biglycan, lumican, and fibromodulin. FASEB J. 2001; 15:559–561. [PubMed: 11259366]

Schaefer L, Schaefer RM. Proteoglycans: from structural compounds to signaling molecules. Cell Tissue Res. 2010; 339:237–246. [PubMed: 19513755]

Schall TJ, Bacon K, Toy KJ, Goeddel DV. Selective attraction of monocytes and T lymphocytes of the memory phenotype by cytokine RANTES. Nature. 1990; 347:669–671. [PubMed: 1699135]

Sjoberg AP, Manderson GA, Morgelin M, Day AJ, Heinegard D, Blom AM. Short leucine-rich glycoproteins of the extracellular matrix display diverse patterns of complement interaction and activation. Mol Immunol. 2009; 46:830–839. [PubMed: 18962898]

Tesch GH. MCP-1/CCL2: a new diagnostic marker and therapeutic target for progressive renal injury in diabetic nephropathy. Am J Physiol Renal Physiol. 2008; 294:F697–701. [PubMed: 18272603]

Westergren-Thorsson G, Hernnas J, Sarnstrand B, Oldberg A, Heinegard D, Malmstrom A. Altered expression of small proteoglycans, collagen, and transforming growth factor-beta 1 in developing bleomycin-induced pulmonary fibrosis in rats. J Clin Invest. 1993; 92:632–637. [PubMed: 7688761]

Wu H, Chen G, Wyburn KR, Yin J, Bertolino P, Eris JM, Alexander SI, Sharland AF, Chadban SJ. TLR4 activation mediates kidney ischemia/reperfusion injury. J Clin Invest. 2007; 117:2847–2859. [PubMed: 17853945]

Xu T, Bianco P, Fisher LW, Longenecker G, Smith E, Goldstein S, Bonadio J, Boskey A, Heegaard AM, Sommer B, Satomura K, Dominguez P, Zhao C, Kulkarni AB, Robey PG, Young MF. Targeted disruption of the biglycan gene leads to an osteoporosis-like phenotype in mice. Nat Genet. 1998; 20:78–82. [PubMed: 9731537]

Young MF, Bi Y, Ameye L, Chen XD. Biglycan knockout mice: new models for musculoskeletal diseases. Glycoconj J. 2002; 19:257–262. [PubMed: 12975603]

Highlights

- We generated a transient transgenic mouse model where biglycan was overproduced by hepatocytes
- Fully-glycanated biglycan was efficiently synthesized and released into the circulation
- Circulating biglycan targeted the kidneys where it caused recruitment of leukocytes
- Biglycan differentially triggered chemoattraction of leukocytes via Toll-like receptors 2/4
- Leukocytic chemoattraction was mediated by either MyD88 or TRIF adaptor proteins

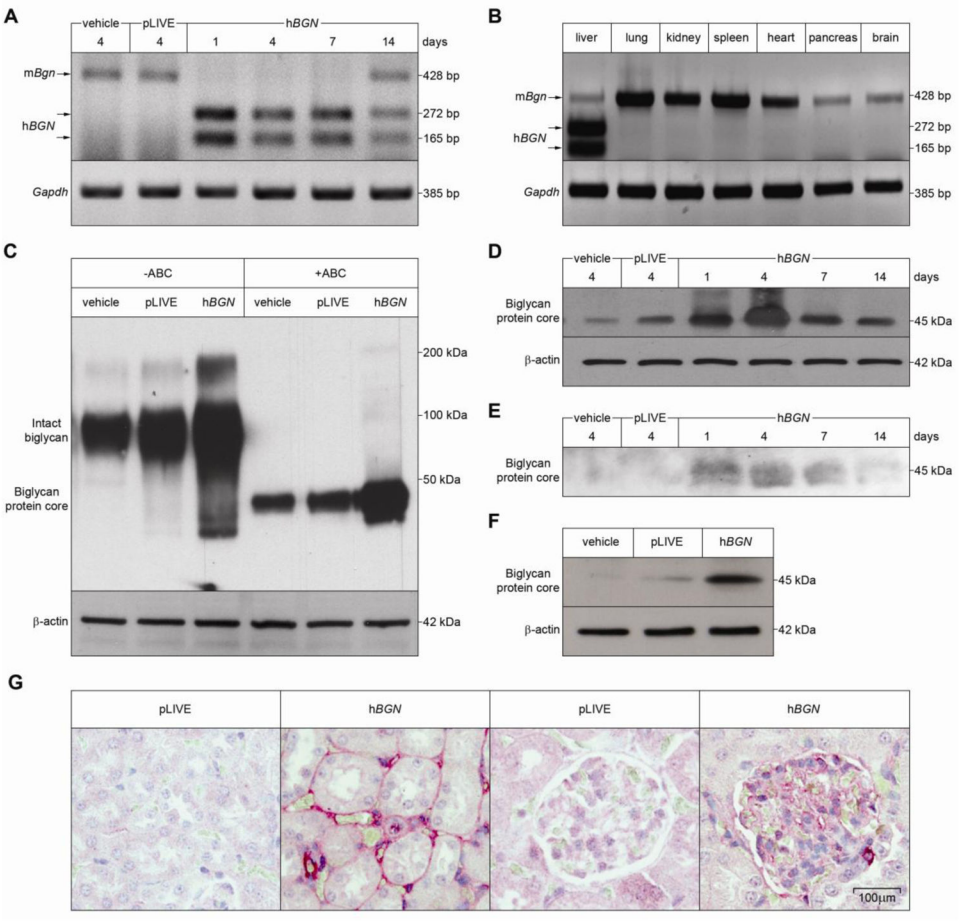

Fig. 1. Liver-specific overexpression of soluble human biglycan (h*BGN*) in mice and its release to the plasma and distribution to the kidney

(**A–B**) RT-PCR-RFLP assay of mRNA extracted from the liver (**A**) or from different organs (**B**) of mice at the indicated time after injection with control or pLIVE-h*BGN* (**A**) or at 4 days after pLIVE-h*BGN* injection (**B**). *Sac*I digestion of amplified cDNA shows two bands at 272 bp and 165 bp for mice expressing h*BGN* and a single band at 428 bp for endogenous mouse biglycan. (**C**) Western blot for human biglycan in the liver of control and pLIVE-h*BGN* injected mice. Chondroitinase ABC digestion results in cleavage of the intact proteoglycan molecule. (**D**) Time course of human biglycan expression in liver of control and pLIVE-h*BGN* injected mice as shown by Western blot. (**E, F**) Western blot of human biglycan isolated from plasma samples (**E**) collected from mice at the indicated time after injection of control or pLIVE-h*BGN* and in mouse kidneys (**F**) collected at 4 days after injection of control or pLIVE-h*BGN*. Samples in D–F were subjected to chondroitinase ABC digestion. (**G**) Immunohistochemical staining for human biglycan in kidneys collected from mice 4 days after injection of pLIVE or pLIVE-h*BGN*.

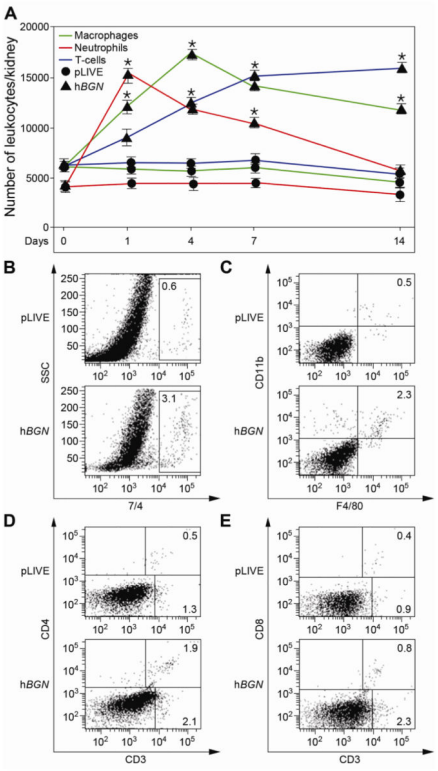

Fig. 2. Flow cytometric analysis of leukocyte infiltrates in kidneys of pLIVE-h*BGN* injected mice

(**A**) Temporal evolution of the number of neutrophils, macrophages and T-cells per kidney of pLIVE and pLIVE-h*BGN* injected mice as determined by FACS. (**B–E**) Percentage of 7/4+ cells (**B**), F4/80+CD11b+ (**C**), CD3+ (**D–E**), CD3+CD4+ (**D**), and CD3+CD8+ (**E**) cells in kidneys of pLIVE and pLIVE-h*BGN* injected mice at 1 (**B**), 4 (**C**) and 7 (**D–E**) days post injection. Data are presented as mean ± SEM; n=3.

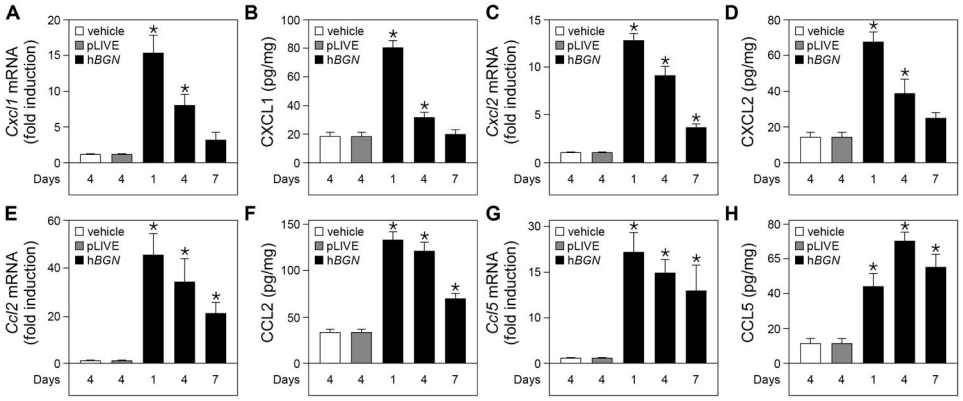

Fig. 3. Increased chemokine mRNA and protein levels in mouse kidney following pLIVE-h*BGN* injection

(**A, C, E, G**) qPCR analysis of mRNA levels of *Cxcl1* (**A**), *Cxcl2* (**C**), *Ccl2* (**E**), *Ccl5* (**G**) in kidneys of control or pLIVE-h*BGN* injected mice. (**B, D, F, H**) Protein levels of CXCL1 (**B**), CXCL2 (**D**), CCL2 (**F**), CCL5 (**H**) in kidneys of control or pLIVE-h*BGN* injected mice as determined by ELISA. mRNA levels are presented as relative to that of *Gapdh*. The time elapsed between injection and sample collection is indicated under each bar. Data are presented as mean ± SEM, n=4.

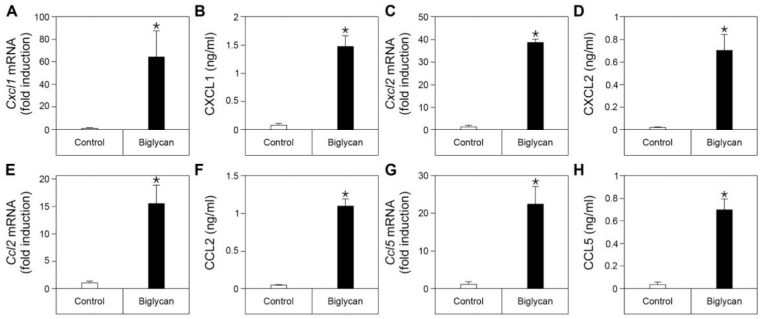

Fig. 4. Increased chemokine mRNA levels and protein secretion in mouse peritoneal macrophages stimulated with biglycan

(**A, C, E, G**) qPCR analysis of mRNA levels of *Cxcl1* (**A**), *Cxcl2* (**C**), *Ccl2* (**E**), *Ccl5* (**G**) in mouse peritoneal macrophages 4 h after stimulation with biglycan (4 μg/ml). (**B, D, F, H**) Secreted protein levels of CXCL1 (**B**), CXCL2 (**D**), CCL2 (**F**), CCL5 (**H**) in culture media of mouse peritoneal macrophages 16 h after stimulation with biglycan (80 nM) as determined by ELISA. Data are presented as mean ± SD, n=4.

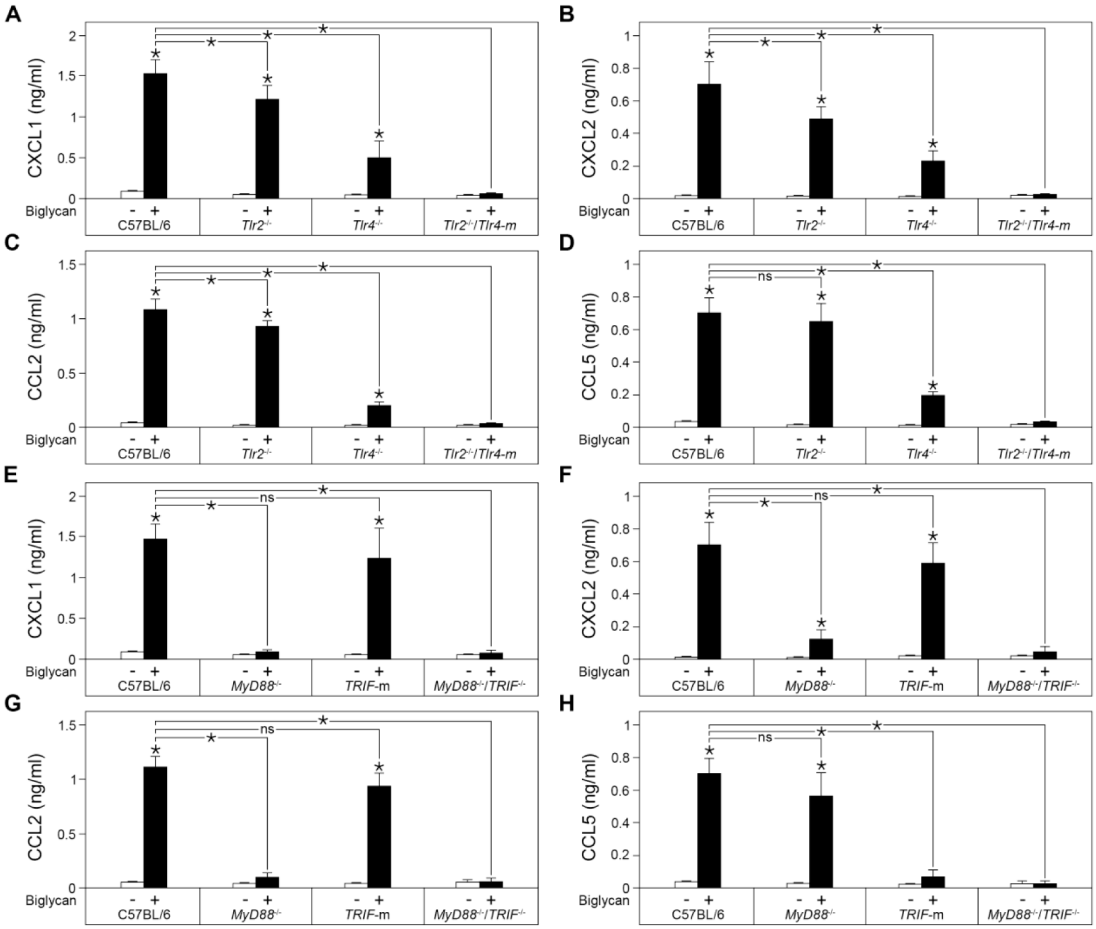

Fig. 5. Chemokine secretion profile of biglycan-stimulated peritoneal macrophages collected from C57BL/6, *Tlr2*$^{-/-}$, *Tlr4*$^{-/-}$, *Tlr2*$^{-/-}$*Tlr4-m*, *MyD88*$^{-/-}$, *TRIF-m* and *MyD88*$^{-/-}$ *TRIF*$^{-/-}$ mice

(**A–D**) Secreted protein levels of CXCL1 (**A**), CXCL2 (**B**), CCL2 (**C**), CCL5 (**D**) in the culture medium of mouse peritoneal macrophages collected from C57BL/6, *Tlr2*$^{-/-}$, *Tlr4*$^{-/-}$ and *Tlr2*$^{-/-}$*Tlr4-m* mice 16 h after stimulation with biglycan (4 μg/ml) as determined by ELISA. (**E–H**) Secreted protein levels of CXCL1 (**E**), CXCL2 (**F**), CCL2 (**G**), CCL5 (**H**) in culture media of mouse peritoneal macrophages collected from C57BL/6, *MyD88*$^{-/-}$, *TRIF-m* and *MyD88*$^{-/-}$*TRIF*$^{-/-}$ mice 16 h after stimulation with biglycan (80 nM) as determined by ELISA. Data are presented as mean ± SD, n=4; ns=not significant.

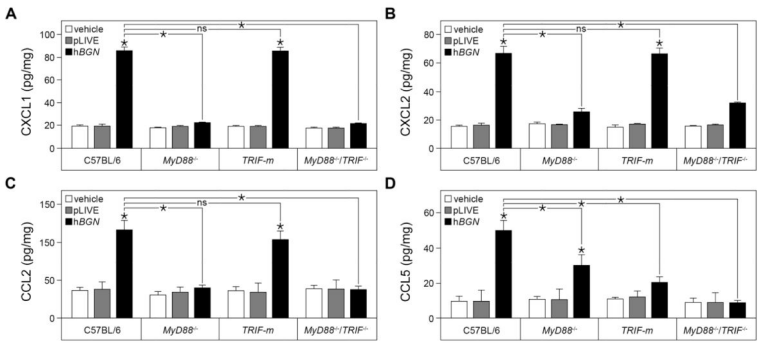

Fig. 6. Renal chemokine levels following pLIVE-h*BGN* injection in C57BL/6, *MyD88*$^{-/-}$, *TRIF-m* and *MyD88*$^{-/-}$*TRIF*$^{-/-}$ mice

(**A–D**) Protein levels of CXCL1 (**A**), CXCL2 (**B**), CCL2 (**C**) and CCL5 (**D**) in mouse kidney as determined by ELISA. Samples were collected from control and pLIVE-h*BGN* injected mice one day (**A, B**), 4 days (**C**) or 7 days (**D**) after injection. Data are presented as mean ± SD, n=4; ns=not significant.

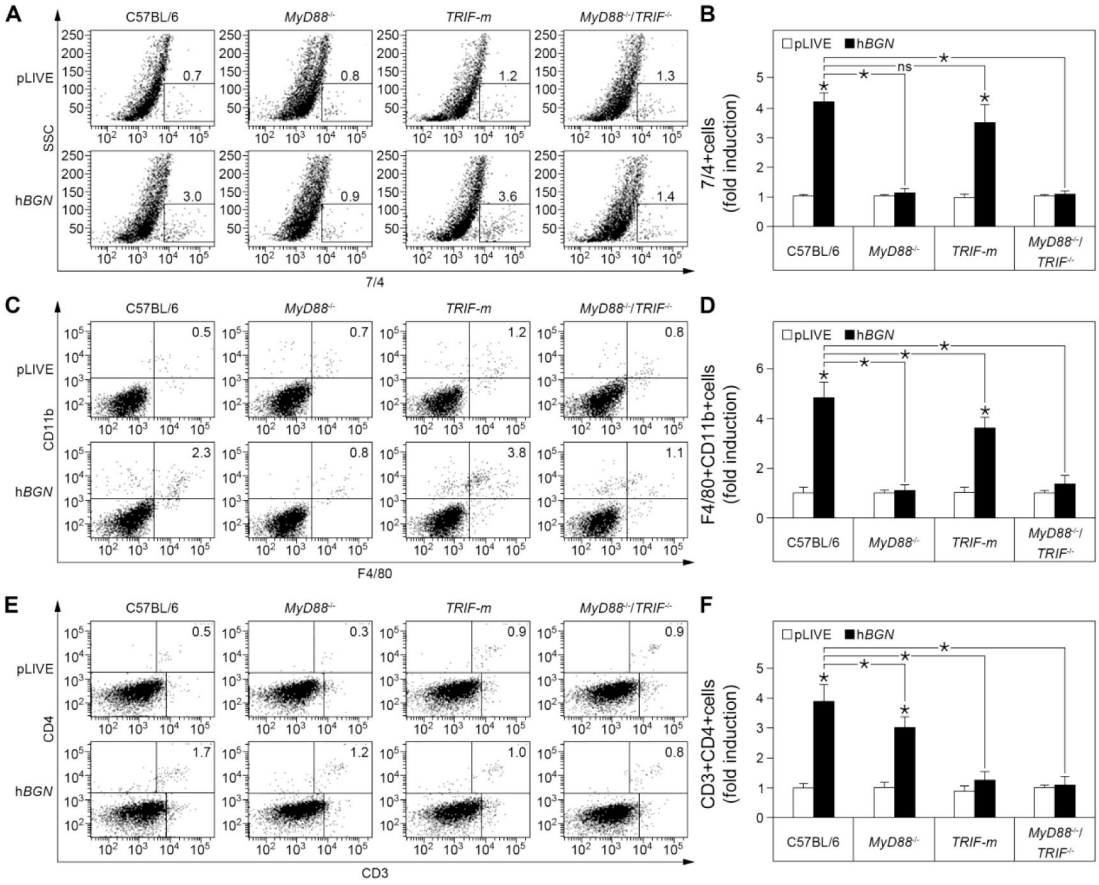

Fig. 7. Flow cytometric analysis of leukocyte infiltrates in kidneys of C57BL/6, *MyD88*$^{-/-}$, *TRIF-m* and *MyD88*$^{-/-}$*TRIF*$^{-/-}$ mice injected with pLIVE-h*BGN*

(**A, C, E**) Percentage of 7/4+ (**A**) CD11b+F4/80+ (**C**) and CD3+CD4+ (**E**) cells in mouse kidney at one day (**A**), 4 days (**C**) or 7 days (**E**) after injection of pLIVE or pLIVE-h*BGN*. (**B, D, F**) Levels of 7/4+ (**B**), CD11b+F4/80+ (**D**) and CD3+CD4+ (**F**) cells in mouse kidney presented as fold induction to the respective controls at one day (**B**), 4 days (**D**) or 7 days (**F**) after injection of pLIVE or pLIVE-h*BGN*. Data are presented as mean ± SD, n=4; ns=not significant.

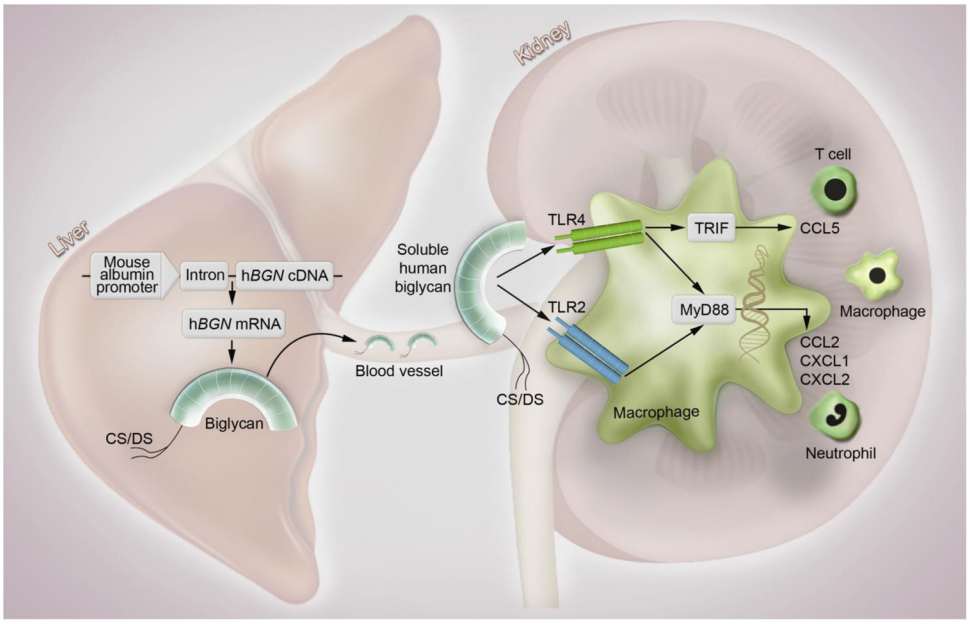

Fig. 8. Mechanism of soluble biglycan-triggered inflammation *in vivo*

The liver-specific overexpression of soluble human biglycan leads to its release into the bloodstream followed by its distribution to the kidneys. Biglycan acts as an endogenous ligand of TLR2 and TLR4 in macrophages and triggers CXCL1, CXCL2 and CCL2 production through the MyD88 pathway and CCL5 production through the TRIF pathway. As a consequence of chemoattractant production, neutrophils, macrophages and T cells are recruited to the kidney. h*BGN*, human biglycan gene; CS/DS, chondroitin sulfate/dermatan sulfate; TLR, Toll-like receptor; TRIF, TIR-domain-containing adapter-inducing interferon-β; CCL2, Chemokine (C-C motif) ligand 2; CCL5, Chemokine (C-C motif) ligand 5; CXCL1, Chemokine (C-X-C motif) ligand 1; CXCL2, Chemokine (C-X-C motif) ligand 2.